JOURNAL OF GEOPHYSICAL RESEARCH, VOL. 94, NO. B12, PAGES 17,793–17,804, DECEMBER 10, 1989

Reflectivity and Seismic Properties of the Deep Continental Crust

NIKOLAS I. CHRISTENSEN

Department of Earth and Atmospheric Sciences, Purdue University, West Lafayette, Indiana

The recovery of drill core from a section of upper amphibolite facies terrane located in the Inner Piedmont of South Carolina provides a rare opportunity to study in detail the seismic character of rocks which were once part of the deep continental crust. Seismic reflection profiles over the Inner Piedmont in the vicinity of the drill hole reveal subhorizontal high-amplitude reflections. The origin of these reflections has been investigated by measuring compressional wave velocities as a function of confining pressure and densities in 150 samples obtained from 305 m of drill core. Synthetic seismograms generated from the velocity and density measurements demonstrate that reflections originate from subhorizontal metamorphic layering, probably originating from lower crustal ductile flow. Fine tuning of the metamorphic layering, which is temperature and pressure related, can produce bright spots in the deep crust. Anisotropy, resulting from preferred mineral orientation, is another important property of this section. Velocities are low for vertical wave propagation, whereas horizontal velocities are relatively high. Horizontal velocities show only a slight variation with azimuth, which is unlikely to be detected using standard refraction techniques. Reflectivity decreases with increasing anisotropy. Critical to this study has been the continuous coring of a major section of high-grade metamorphic terrane, which has provided the necessary stratigraphic and lithologic control for the generation of accurate synthetic seismograms.

Author's Personal Copy

INTRODUCTION

During the past decade, much progress has been made toward an improved understanding of the seismic properties of the deep continental crust. Seismic reflection profiling has produced significant new information on crustal structure. High-resolution refraction data and new computer modeling techniques have provided detailed velocity resolution of the crust. These studies offer exciting new perspectives on the origin, evolution, and composition of the continental crust.

The application of high-resolution seismic techniques to the deep continental crust has raised many questions concerning the geological interpretation of seismic data. Although many origins have been proposed for the observed reflectivity of crustal sections, the nature of crustal reflectors is still highly speculative. Composition is often inferred from refraction velocities. Most velocities reported for deep crustal regions, however, can originate from a wide variety of igneous and metamorphic rock types or, more realistically, complex assemblages of several rock types. Anisotropy originating from preferred mineral orientation associated with extensional or compressional lower crustal ductile flow undoubtedly complicates both crustal reflection and refraction data, although analyses of crustal seismic data usually assume isotropic elasticity. Clearly, the geologic interpretation of crustal seismic data represents an important frontier in the earth sciences and is complicated by the structural and compositional heterogeneity inherent to the continental crust.

This study deals with the seismic properties of the deep continental crust and their geologic interpretation. Detailed seismic properties are presented for a 300-m section of high-grade metamorphic rocks originating within the lower continental crust. Discussion concentrates on the origin of reflections from this section using synthetic modeling and the overall velocity structure of this section and its correlation with metamorphic petrology. Topics to be addressed include (1) the origin of deep crustal reflectors, (2) the relationship of crustal petrology to seismic velocities, (3) the nature of crustal seismic anisotropy, and (4) deep crustal bright spots.

Copyright 1989 by the American Geophysical Union.

Paper number 89JB02979.
0148-0227/89/89JB-02979$05.00

SEISMIC PROPERTIES OF A DEEP CRUSTAL SECTION

In 1985 the National Science Foundation sponsored a site investigation for an ultradeep scientific core hole in the southern Appalachians [*Williams et al.*, 1987]. This project included geologic mapping, shallow drilling at four sites, and seismic reflection profiling. The reflection profiles were acquired from the eastern Blue Ridge across the Brevard fault zone and Chauga belt into the Inner Piedmont (Figure 1). The seismic studies, which are of extremely high quality for data from a continental crystalline terrane, reveal much detail on the structural geometry of the Blue Ridge-Piedmont thrust sheet [*Coruh et al.*, 1987; *Hatcher et al.*, 1987]. Of particular interest for the present study are the reflectors observed within the Inner Piedmont (Figure 2). One of the drill sites (DH-1, Figure 1) was located on the northwestern flank of the Inner Piedmont of northwestern South Carolina. Drilling at this site penetrated 305 m of upper amphibolite facies crystalline rock with nearly 100% recovery. Because of its continuity and unweathered nature, the drill core has provided a unique opportunity to study the seismic properties of a continuous section of metamorphic rock originating in the deep continental crust. An earlier study of seismic properties from hole DH-2, located within the Brevard fault zone, has provided information on the origin of fault zone reflectivity [*Christensen and Szymanski*, 1988].

The Precambrian Inner Piedmont in this region consists of a variety of lithologies, which are typical of many high-grade metamorphic terranes throughout the world. Within the drill core, three major rock types were sampled: (1) granitic gneiss, (2) biotite quartzofeldspathic gneiss, and (3) amphibolite. The rocks are usually separated by sharp contacts, which vary in attitude from horizontal to dips rarely in excess of 20°. Foliation, due to preferred orientation of quartz, amphibole, and mica, is often well developed and usually parallel to lithologic contacts. Important mineralogical variations occur within each major rock type which are significant in terms of seismic velocities and densities. The granitic gneisses, which are chemically equivalent to low potassium granites, are typically medium grained biotite-bearing gneisses with abundant feldspar and quartz. Garnet and muscovite are often present. The biotite quartzofeldspathic gneisses, which probably were derived from a metasedimentary protolith, show the most variability. Hornblende and garnet, when abundant, increase velocities. Kyanite and/or sillimanite are often present. The rocks

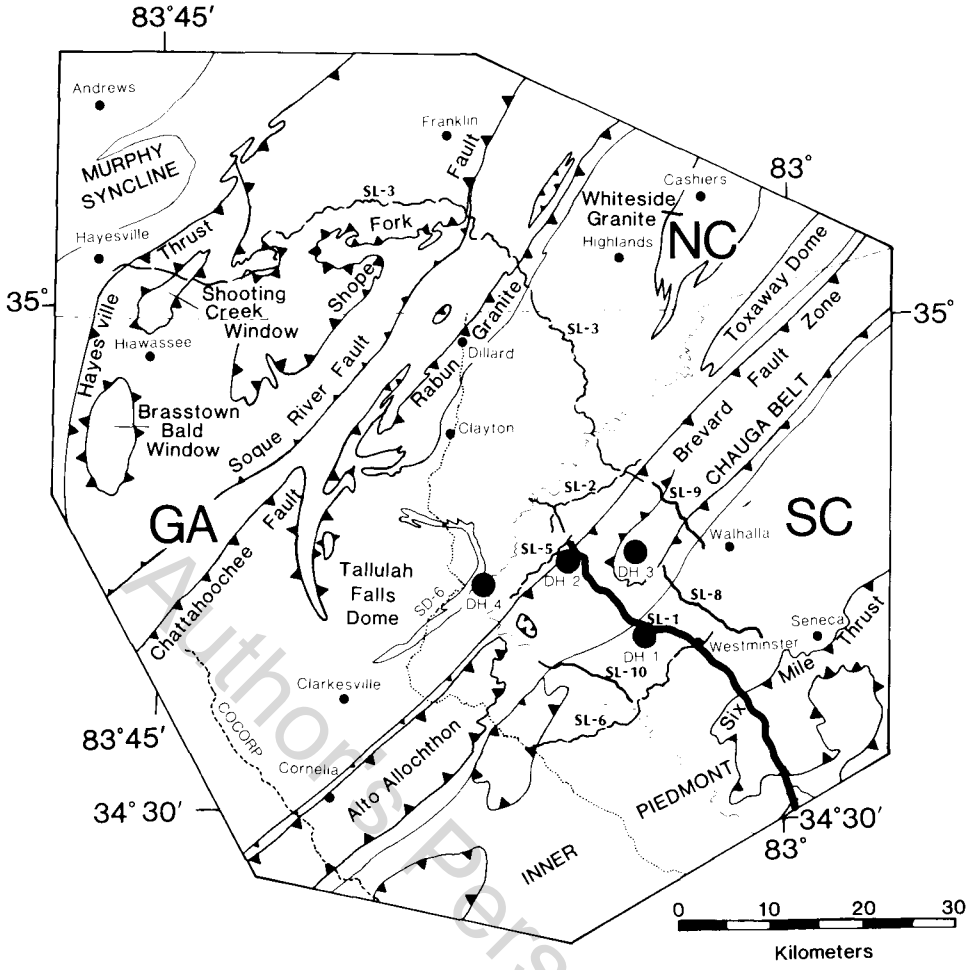

Fig. 1. Map showing locations of core holes (DH-1-DH-4), seismic reflection lines, and major structural features. Heavy line indicates the location of seismic line SL-1 of Figure 2 [from *Hatcher et al.*, 1987].

with the highest velocities are the amphibolites which contain andesine and hornblende along with variable amounts of quartz, biotite, epidote and garnet. Up to 20% pyroxene is present locally in the amphibolites, suggesting that some samples approach lower granulite facies grade. A detailed description of the drill core by *Farrar et al.* [1986] is summarized in Figure 3 and average modal analyses are given in Table 1. The PT conditions under which the Piedmont drill core rocks formed have not been accurately determined; however, their mineralogy places their origin at mid to lower crustal depths.

Representative samples were collected at closely spaced intervals for velocity and density measurements. Fifty sections of core were selected, with an average spacing of 6.1 m. From the core sections, 150 minicores (4-6 cm in length and 2.5 cm in diameter) were cored, trimmed, and jacketed for compressional wave velocity measurements as a function of pressure. To investigate seismic anisotropy, three cores (designated A, B, and C) were taken from each sample. The axes of the A cores were oriented normal to foliations (i.e., approximately vertical), and the B and C cores were cut perpendicular to one another with their axes in the foliation planes. When lineations were observed, the axes of the B cores were oriented parallel to the lineations. Bulk densities of the minicores were calculated from their weights and dimensions.

Table 2 gives the velocities for the A and B cores to crustal depths of approximately 35 km, measured using a pulse transmission technique [*Birch*, 1960]. At a given depth, the lowest velocities were consistently measured for the A cores (i.e., with propagation normal to foliations). For many depth intervals, the B and C core velocities were within a few percent of one another,

TABLE 1. Average Modal Analyses

Mineral	Granitic Gneiss (22 Samples)	Biotite Quartzofeldspathic Gneiss (10 Samples)	Amphibolite (18 Samples)
Microcline	35.4	-	-
Plagioclase	33.7	55.2	38.8
Quartz	24.5	25.1	6.9
Muscovite	1.4	-	-
Biotite	3.0	16.3	2.6
Hornblende	-	0.9	47.6
Pyroxene	-	-	2.5
Garnet	0.8	1.2	-
Epidote	-	-	1.1
Magnetite	1.2	1.3	0.5

Values are in volume percent.

Author's Personal Copy

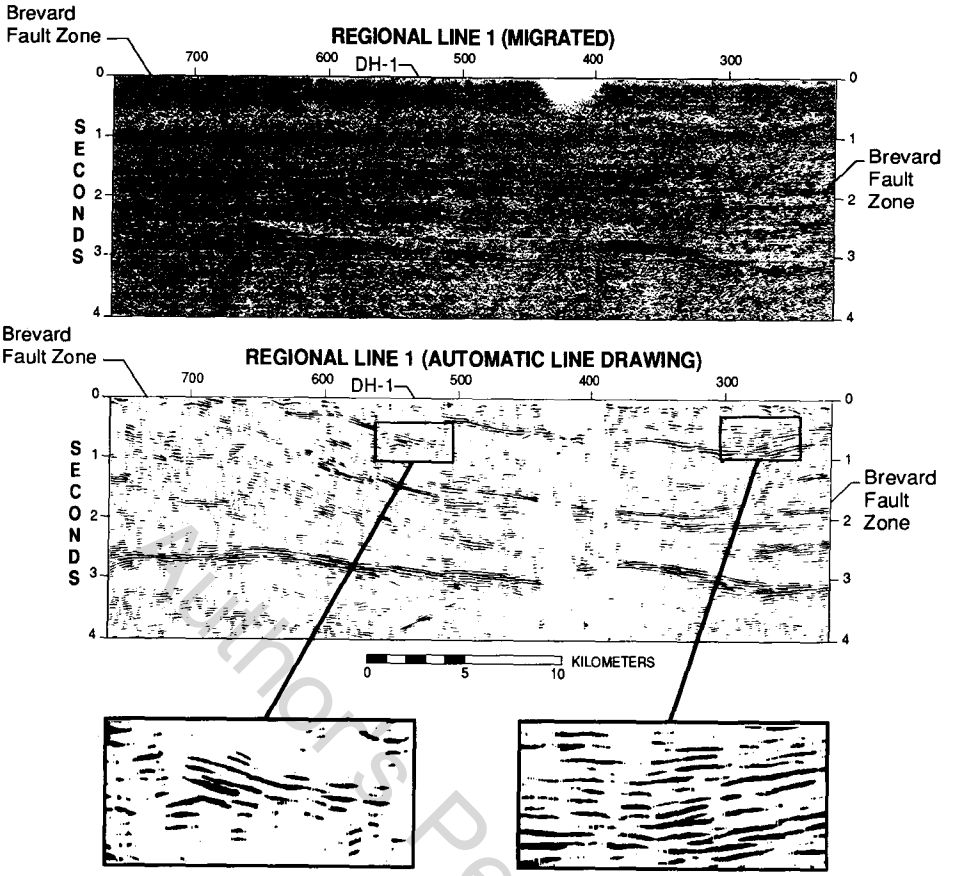

Fig. 2. ADCOH line 1. Inner Piedmont reflectors are located above Brevard fault zone. The strong reflections at approximately 3.0 s are interpreted as originating from a lower Paleozoic sedimentary sequence [from *Williams et al.*, 1987; *Costain et al.*, 1989]. The reflective character of two Inner Piedmont regions are enlarged in the lower portion of the figure.

Author's Personal Copy

which is similar to findings of earlier studies of seismic anisotropies of schists and gneisses [*Birch*, 1960; *Christensen*, 1965]. Exceptions are some amphibolite velocities, which are significantly higher for B cores, due to the preferred alignment of fast hornblende *c* crystallographic axes in the foliation planes and parallel to lineations [*Christensen*, 1965]. Thus the data in Table 2 give maximum anisotropies at the selected depth intervals.

Reflectivity of the Deep Crust

The interlayering of the drill hole rocks suggests that a layered source geometry may be responsible for the Inner Piedmont reflections. Based on visual examination of the drill core and the descriptions of *Farrar et al.* [1986], the 305 m section has been divided into 153 layers, varying in thickness from 0.3 to 13.7 m. Using the measured velocities (Table 2) and visual and petrographic examinations of the core, velocities and densities were assigned to each layer for reflectivity modeling. A time series containing reflection coefficient information is constructed from the layer thicknesses, velocities, and densities. This series is convolved with a zero-phase, three-extrema 30-Hz wavelet to produce the seismograms. Although the seismograms consider transmission losses at each interface, no attempt is made to account for dispersion, geometrical spreading, attenuation, or multiple reflections. For clarity, the signal-to-noise ratio is infinite. Layering is assumed to be horizontal. This is consistent with models of deep crustal sections based on surface exposures of high-grade metamorphic terranes [e.g., *Coward*, 1973; *Park*, 1981; *Percival and Card*, 1983]. The development of horizontal structures has usually been attributed to prograde metamorphism associated with crustal thickening at convergent plate boundaries [*Newton*, 1987; *Bois et al.*, 1987] or ductile flow accompanying crustal extension [*Sandiford and Powell*, 1986].

Each synthetic seismogram follows the same format. The vertical axis is total two-way travel time in seconds. The leftmost trace, labeled "D," is a depth scale with tic marks at 50 m intervals. Since the depth is a function of two-way travel time and velocity, the scale is nonlinear. The velocity model "V" gives the variation in velocity with depth. "RHO" displays the densities used to calculate the synthetic traces. The "RC" trace shows the reflection coefficient series, with spikes to the right indicating positive acoustic impedance contrasts. "SYN" is the resulting synthetic seismogram, which is shown seven times to simulate a segment of a zero-offset two-dimensional seismic record. For comparison, a standard trace, "ST," is shown which corresponds to a model consisting of a +0.1 reflection coefficient interface, comparable to that of a sandstone-limestone contact in a sedimentary sequence. By comparing the amplitudes of the model reflections to the standard trace, one can better appreciate the magnitudes of the reflections in the synthetic seismograms. A 0.1 reflection coefficient is characteristic of a strong reflector, whereas fair reflections originate from rock interfaces with reflection coefficients of 0.04 [*Sheriff*, 1975]. For comparison, the reflection

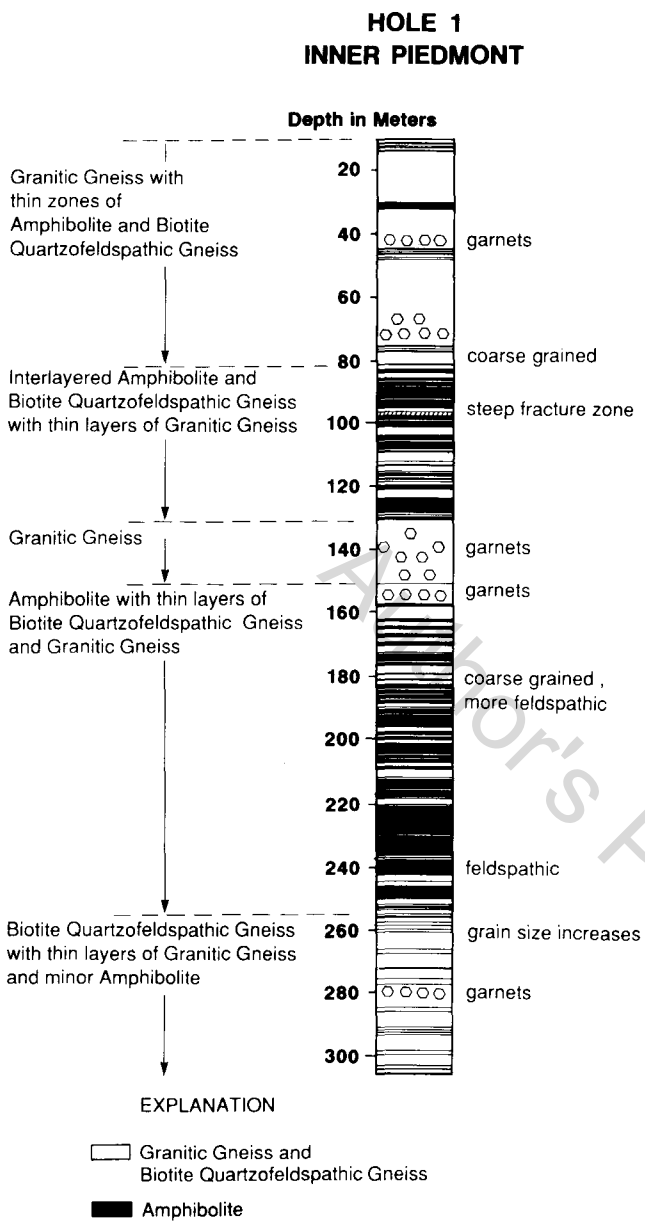

Fig. 3. Summary of DH-1 petrology [after *Farrar et al.*, 1986].

coefficient at 1 GPa and 500C of a garnet granulite-lherzolite contact, which is likely to give rise to observed reflections from the Mohorovicic discontinuity, is of the order of 0.07.

Figures 4 and 5 show synthetic reflection traces calculated from velocities measured at 200-MPa confining pressure for the Inner Piedmont section. Figure 4, which was obtained using A core velocities and densities, is appropriate for a near-vertical incidence reflection survey. It is clear from reflections generated in this seismogram that the metamorphic layering observed in hole DH-1 produces significant reflections.

Figure 5 compares the synthetic seismogram of Figure 4 with a trace calculated using the mean velocities and densities of the A, B, and C cores. The reflections result from a layered geometry identical to that of Figure 4; however, each layer is isotropic. Isotropic velocities were obtained by averaging the three mutually perpendicular velocities for each layer. The amplitude factor in Figure 5 has been increased to better separate the two reflection traces. Although the synthetic seismograms of the anisotropic and isotropic models are similar, the isotropic model amplitudes are greater. Thus the anisotropy inherent to the metamorphic rocks of the Inner Piedmont reduces reflectivity. The petrologic explanation for this observation is quite simple. The rocks with the highest velocities and anisotropies are the amphibolites. When the amphibolite foliation has a subhorizontal orientation, velocities measured in the vertical direction are slow. Hence reflection coefficients at amphibolite-biotite quartzofeldspathic gneiss and amphibolite-granite gneiss interfaces are lowered by the presence of anisotropy. Reflection coefficients for the isotropic model average 0.03 greater than the anisotropic model and reach a maximum of 0.14.

The lowering of reflectivity by anisotropy is surprising and at first seems contradictory to the previous finding that anisotropy increases reflectivity of the Brevard Fault Zone drill core [*Christensen and Szymanski*, 1988]. However, the rocks of the Brevard Fault Zone are quite different from those of the Inner Piedmont section. Within the Brevard Fault Zone, variations in the percentage of anisotropy with depth of silicic mylonites produce reflections. The Inner Piedmont section, on the other

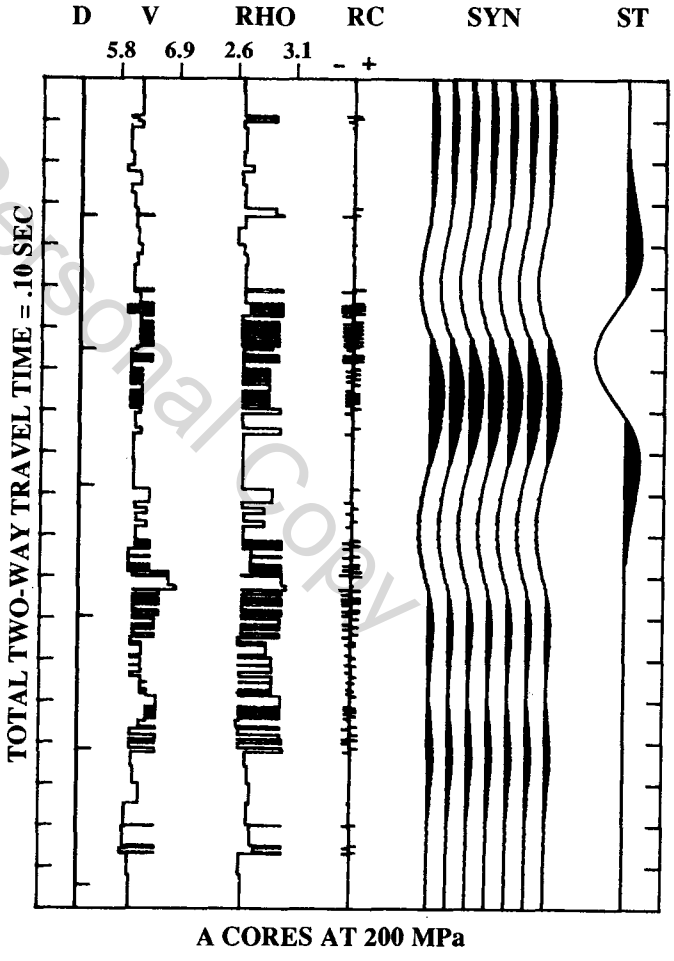

Fig. 4. Reflection synthetic from Inner Piedmont A cores at 200 MPa. The vertical axis is total two-way travel time in seconds. The trace labeled "D" is a depth scale in 50 m intervals. The trace labeled "V" is the velocity model in km s^{-1}, and "RHO" is the density model in kg m^{-3} x 10^{-3}. "RC" is the reflection coefficient series with excursions to the right representing positive acoustic impedance contrasts. "SYN" is the synthetic seismogram consisting of seven identical traces. A standard trace ("ST"), consisting of a +0.1 reflection coefficient interface, is provided for amplitude comparison.

Author's Personal Copy

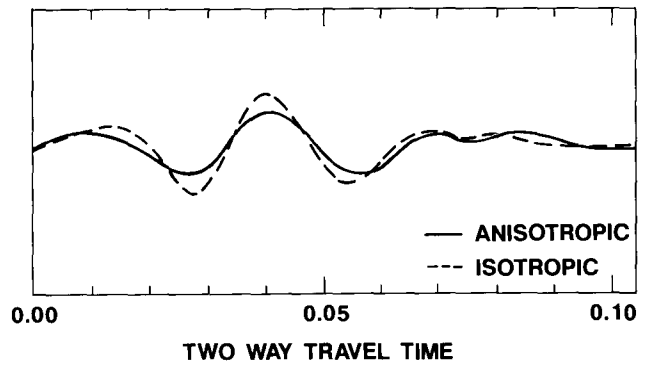

Fig.5. Reflections originating from a hypothetical isotropic Inner Piedmont section compared to the anisotropic section of Figure 4.

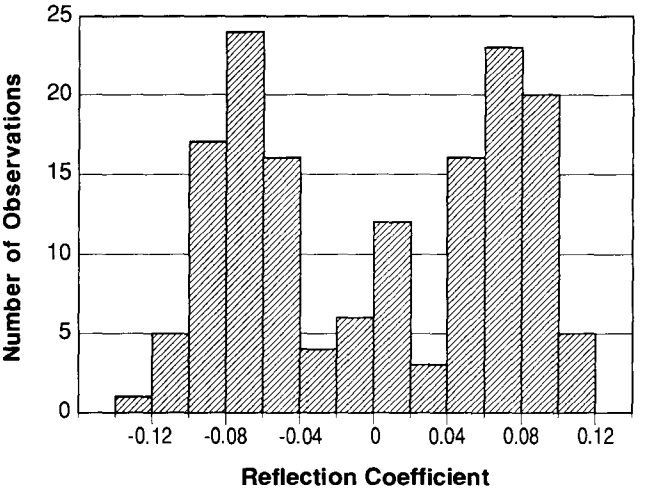

Fig. 6. Reflection coefficients determined for the Inner Piedmont section at confining pressures of 200 MPa.

hand, consists of alternating felsic gneisses and mafic amphibolites.

The modeling results demonstrate the important contribution of metamorphic layering to deep crustal reflectivity. The role of layering in producing reflections was first suggested by *Fuchs* [1969] and has recently been emphasized in several discussions of the origin of crustal reflections [e.g., *Hale and Thompson*, 1982; *Jones and Nur*, 1984; *Hurich et al.*, 1985; *Smithson et al.*, 1986; *McCarthy*, 1986; *Matthews and Cheadle*, 1986; *Meissner*, 1986]. Undoubtedly, the reflectivities of layered metamorphic rock sequences are complex. Layer thicknesses are critical as well as wavelet frequencies. The metamorphic layering observed and modeled for the Inner Piedmont section is much thinner than the optimum quarter wavelength thickness often cited in the production of strong reflections in laminated media [*Fuchs*, 1969].

The average layer thickness of the Inner Piedmont section is 2.1 m. The minimum and maximum layer thicknesses of 0.3 and 13.7 m are relatively thin compared to wavelengths of reflections from the deep crust, which usually are in the range of 200-700 m. Modeling of thin layer reflectivity by *Widess* [1973] has shown that the reflection amplitude approximates $4\pi Ab/\lambda$, where A is the reflection amplitude for a very thick layer, b is the layer thickness, and λ is the wavelength. Thus a layer of only a few meters thickness can have significant reflective power for typical frequencies and velocities.

Model studies of layered sequences [e.g., *Velzeboer*, 1981; *Hurich and Smithson*, 1987] have provided much information on the role of layer thickness in producing constructive and destructive interference. An analysis of the magnitude of reflections by *Hurich and Smithson* [1987] for a layered crustal section consisting of uniformly thick layers with reflection coefficients oscillating between + and -0.04 demonstrated that constructive interference is limited to a relatively narrow range of layer thicknesses. Constructive interference was shown to be significant for layer thicknesses between 80 and 35 m for typical seismic frequencies, whereas layers thinner than 35 m produced amplitudes less than that of a single boundary, indicating destructive interference. Since layer thicknesses are highly variable (Figure 4) and the reflection coefficients show a wide range of values (Figure 6), reflectivity of the Inner Piedmont section is more complex.

Because of constraints imposed by a single drill hole, modeling of the Inner Piedmont section is limited to one dimension. The continuities of the layers as well as lateral variations in fabrics are unknowns, which undoubtedly are of major importance in understanding the observed reflectivity of a region [*Blundell and Raynaud*, 1986; *Goodwin and Thompson*, 1988]. Reflections in some localities within the Inner Piedmont appear to be continuous for distances up to several hundred meters (Figure 2), suggesting that locally layering similar to that observed in the drill hole may have comparable lateral extents.

The reflectivity observed within the Inner Piedmont section highlights the problem of attempting to model crustal reflectivity from limited velocity-density data and poor structural control. Reflectivity of the Inner Piedmont section is calculated in Figures 7, 8, and 9 assuming that samples were collected at 30-, 15-, and

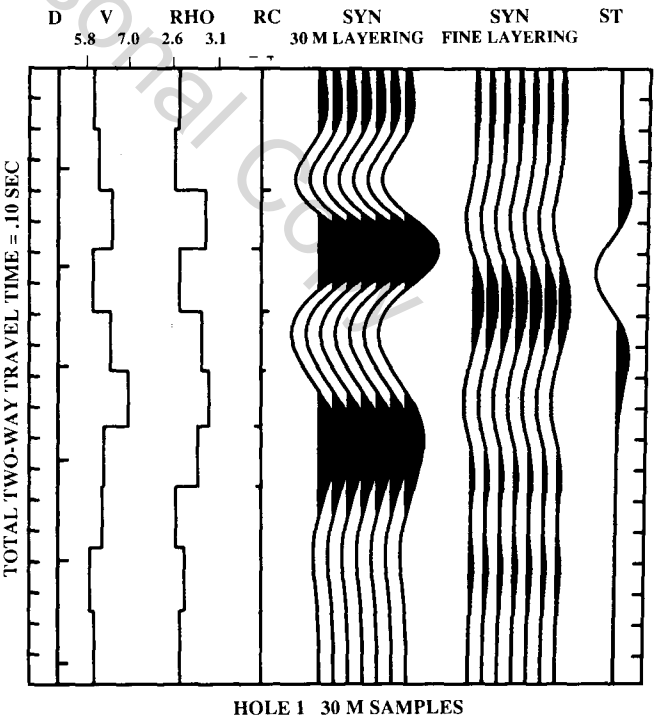

Fig. 7. Reflectivity of the Inner Piedmont section calculated for a 30 m sample spacing. The reflection synthetic assumes no knowledge of the fine structure of the section and is calculated from A core 200 MPa velocities and densities at 30 m intervals. For comparison, the calculated reflectivity of Figure 4 is shown on the right. For details of plot structure, refer to Figure 4 caption and text.

For Personal Copy

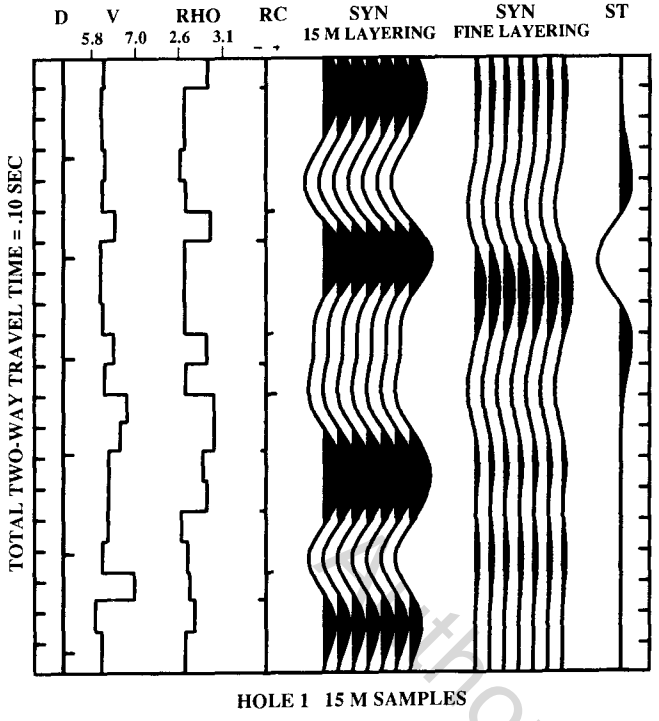

Fig. 8. Reflectivity of the Inner Piedmont section calculated for a 15 m sample spacing compared with the reflectivity calculated in Figure 4.

7.5-m intervals. Thirty hertz wavelets are used for each seismogram, as well as A core velocities measured at 200 MPa. Comparisons of these synthetic seismograms with the reflectivity calculated in Figure 4 demonstrate important limitations of reflection modeling. For the Inner Piedmont section a reasonable reflection synthetic is not generated until the sample spacing approaches 7.5 m. At 30 Hz and an average velocity of 6.6 km/s, the wavelength is 220 m. Sampling is required at an interval spacing of approximately 4% of the wavelength. Thus conclusions on the origin of crustal reflections based on modeling, using velocity measurements from limited surface exposures in complex metamorphic terranes, are subject to significant error. Understanding continental crustal reflectivity via modeling requires stratigraphic control offered by continuous surface exposures or drill core coupled with a detailed knowledge of rock acoustic impedances.

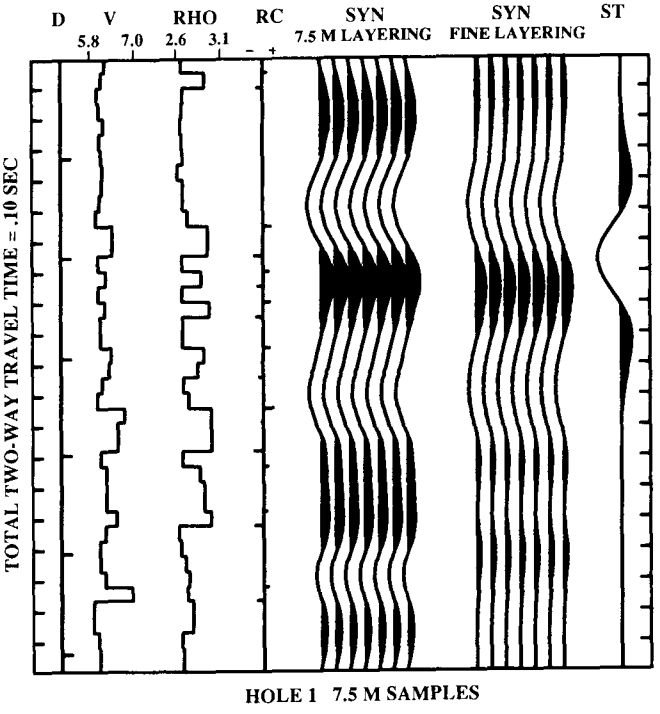

Fig. 9. Reflectivity of the Inner Piedmont section calculated for a 7.5 m sample spacing compared with the reflectivity calculated in Figure 4.

DEEP CRUSTAL BRIGHT SPOTS

The term "bright spot" originated in the petroleum industry to describe high-amplitude reflections in sedimentary sequences, often originating from gas-filled pore space in sandstones. Velocities in water-saturated sands are usually similar to interlayered shales, so reflection coefficients are small. Reflection coefficients are, however, increased if the sand is gas-filled. Strong reflections can also originate from a phase boundary between fluids of different densities trapped within porous rock [*Ostrander*, 1984].

A number of bright spots at depths of 10-20 km have been imaged on deep crustal profiles over crystalline terranes of the United States, Europe, and Australia in regions which have undergone tectonic activity since the Late Paleozoic. Strong reflectors, which lie within recently rifted crust, have been interpreted as originating from magma [*Brown et al.*, 1980]. Other bright spots, however, occur in crystalline basements with no heat

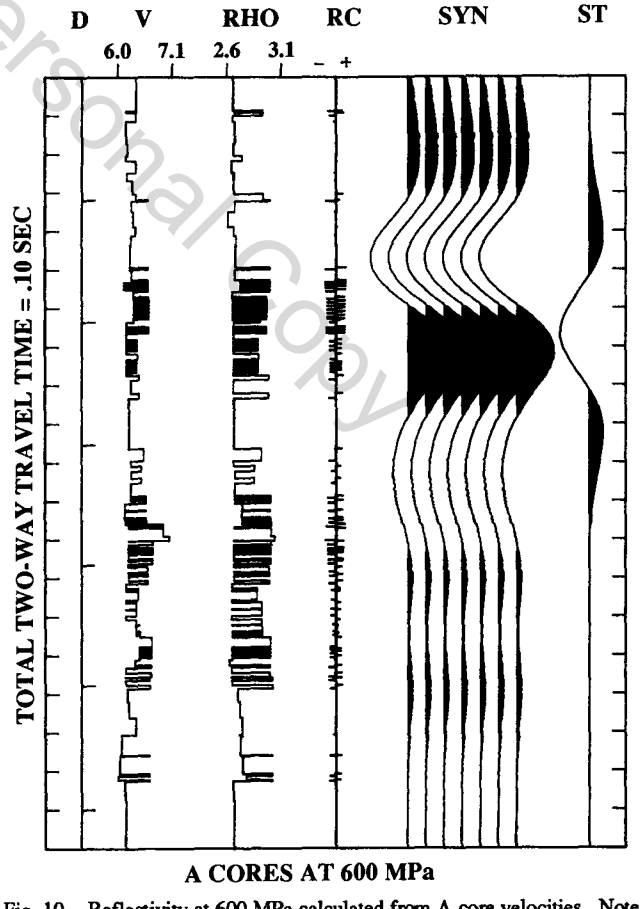

Fig. 10. Reflectivity at 600 MPa calculated from A core velocities. Note the high-amplitude reflections compared with the 200-MPa synthetic of Figure 4.

Author's Personal Copy

TABLE 2. Compressional Wave Velocity as a Function of Pressure

Sample	Depth, m	Orientation	Density, kg m^{-3}	P, MPa 50	100	200	400	600	800	1000
gg	16.5	A	2652	5.54	5.97	6.20	6.30	6.36	6.40	6.43
		B	2651	5.90	6.23	6.37	6.46	6.50	6.54	6.56
gg	21.6	A	2672	5.37	5.79	5.99	6.10	6.16	6.20	6.23
		B	2656	5.98	6.24	6.34	6.42	6.46	6.49	6.51
gg	27.7	A	2656	5.59	5.88	6.04	6.13	6.18	6.21	6.24
		B	2660	5.91	6.13	6.23	6.31	6.35	6.39	6.41
bqg	32.3	A	2734	5.21	5.68	5.94	6.08	6.15	6.21	6.25
		B	2735	5.94	6.28	6.46	6.54	6.58	6.61	6.64
gg	37.8	A	2642	5.33	5.88	6.17	6.29	6.36	6.40	6.44
		B	2637	5.72	6.10	6.25	6.33	6.37	6.40	6.42
gg	41.8	A	2666	5.10	5.70	6.00	6.12	6.18	6.22	6.25
		B	2647	5.72	6.08	6.22	6.28	6.31	6.34	6.36
gg	44.5	A	2661	5.28	5.83	6.06	6.20	6.28	6.33	6.38
		B	2690	5.77	6.11	6.24	6.33	6.38	6.42	6.45
ag	48.5	A	2928	5.20	5.77	6.11	6.27	6.35	6.41	6.45
		B	2883	6.12	6.59	6.84	6.95	7.01	7.05	7.08
gg	52.1	A	2670	5.44	5.91	6.11	6.21	6.27	6.30	6.34
		B	2666	5.65	6.05	6.20	6.28	6.32	6.35	6.37
gg	58.2	A	2610	5.43	5.92	6.14	6.24	6.30	6.34	6.37
		B	2650	6.19	6.25	6.32	6.39	6.44	6.47	6.50
gg	63.1	A	2661	5.78	6.06	6.20	6.30	6.35	6.39	6.42
		B	2656	5.98	6.20	6.30	6.36	6.40	6.42	6.44
gg	66.4	A	2683	5.67	5.99	6.13	6.22	6.26	6.30	6.33
		B	2656	5.95	6.07	6.17	6.26	6.32	6.36	6.39
gg	72.8	A	2674	5.42	5.86	6.07	6.17	6.23	6.28	6.31
		B	2671	5.80	6.10	6.23	6.31	6.35	6.38	6.41
gg	78.9	A	2672	5.59	5.99	6.13	6.21	6.27	6.30	6.33
		B	2659	6.09	6.18	6.25	6.32	6.36	6.39	6.41
bqg	83.8	A	2723	5.22	5.74	5.95	6.06	6.12	6.16	6.19
		B	2720	5.88	6.16	6.27	6.34	6.38	6.41	6.43
ag	86.0	A	2992	5.61	6.16	6.41	6.53	6.60	6.64	6.68
		B	2991	6.75	7.19	7.42	7.52	7.56	7.60	7.62
gg	88.7	A	2649	5.81	6.08	6.19	6.27	6.31	6.34	6.36
		B	2609	5.90	6.08	6.18	6.26	6.31	6.34	6.37
ag	91.4	A	2961	5.56	6.11	6.42	6.55	6.61	6.65	6.69
		B	2917	6.54	6.90	7.11	7.22	7.27	7.30	7.33
ag	100.0	A	2901	5.34	5.89	6.13	6.24	6.31	6.35	6.39
		B	2880	6.67	6.80	6.89	6.98	7.03	7.07	7.09
gg	101.2	A	2660	5.83	5.93	6.02	6.11	6.16	6.20	6.23
		B	2638	5.85	6.18	6.30	6.37	6.41	6.44	6.46
ag	109.7	A	2884	5.63	6.04	6.22	6.33	6.38	6.42	6.45
		B	2844	6.56	6.93	7.11	7.21	7.26	7.29	7.32
ag	116.7	A	2880	5.82	6.11	6.23	6.31	6.37	6.40	6.43
		B	2957	6.19	6.61	6.81	6.91	6.96	6.99	7.02
ag	122.2	A	2980	5.37	5.92	6.21	6.35	6.42	6.47	6.51
		B	2902	6.42	6.54	6.66	6.76	6.81	6.85	6.88
gg	128.6	A	2659	5.53	5.96	6.11	6.20	6.26	6.29	6.32
		B	2649	6.09	6.18	6.26	6.33	6.37	6.40	6.42
gg	135.0	A	2665	5.48	5.92	6.07	6.16	6.21	6.24	6.27
		B	2655	5.90	5.99	6.07	6.17	6.23	6.29	6.33
gg	146.3	A	2664	5.68	5.98	6.09	6.17	6.21	6.25	6.27
		B	2644	5.99	6.19	6.28	6.33	6.36	6.39	6.41
ag	152.1	A	2916	5.93	6.26	6.38	6.47	6.51	6.55	6.58
		B	2921	6.53	6.75	6.89	6.99	7.05	7.09	7.12
ag	159.7	A	2947	6.11	6.24	6.33	6.41	6.46	6.49	6.52
		B	2944	6.58	7.08	7.34	7.45	7.50	7.53	7.56
gg	162.8	A	2673	5.71	6.02	6.13	6.21	6.26	6.29	6.32
		B	2669	5.92	6.16	6.24	6.31	6.35	6.38	6.40
bqg	174.7	A	2739	5.32	5.76	6.00	6.09	6.14	6.17	6.20
		B	2745	6.16	6.23	6.30	6.37	6.42	6.45	6.47
ag	179.8	A	2999	5.87	6.24	6.40	6.50	6.56	6.61	6.64
		B	2955	6.89	7.18	7.32	7.40	7.45	7.48	7.51
ag	186.8	A	3001	6.11	6.54	6.76	6.85	6.90	6.94	6.97
		B	3016	7.32	7.51	7.59	7.66	7.69	7.72	7.74
ag	188.4	A	3038	6.20	6.64	6.86	6.97	7.03	7.07	7.11
		B	3033	7.00	7.43	7.62	7.70	7.75	7.78	7.80

Author's Personal Copy

TABLE 2. (continued)

Sample	Depth, m	Orientation	Density, kg m^{-3}	P, MPa 50	100	200	400	600	800	1000
ag	194.2	A	3002	5.97	6.39	6.56	6.65	6.70	6.73	6.76
		B	2996	6.80	7.19	7.38	7.47	7.52	7.55	7.57
ag	201 .2	A	2988	6.17	6.40	6.48	6.55	6.60	6.63	6.65
		B	2968	6.91	7.29	7.45	7.52	7.56	7.59	7.61
gg	209.1	A	2645	5.60	5.94	6.05	6.12	6.16	6.19	6.21
		B	2636	6.13	6.30	6.36	6.42	6.46	6.48	6.50
ag	212.8	A	2872	5.78	6.11	6.25	6.34	6.40	6.44	6.47
		B	2863	6.85	7.08	7.19	7.25	7.28	7.30	7.32
ag	222.2	A	2920	5.68	6.07	6.24	6.32	6.37	6.40	6.43
		B	2929	6.65	6.88	6.98	7.04	7.07	7.10	7.11
gg	227.7	A	2648	6.05	6.26	6.35	6.40	6.44	6.46	6.48
		B	2647	6.13	6.30	6.37	6.42	6.46	6.48	6.50
ag	235.0	A	2997	5.91	6.36	6.53	6.62	6.67	6.71	6.74
		B	2993	6.74	7.21	7.40	7.48	7.52	7.55	7.57
bqg	242.9	A	2623	5.60	6.04	6.22	6.30	6.35	6.38	6.41
		B	2634	6.07	6.33	6.42	6.48	6.51	6.54	6.56
ag	250.2	A	3018	5.91	6.38	6.52	6.60	6.64	6.67	6.70
		B	3022	7.06	7.37	7.50	7.56	7.59	7.62	7.64
bqg	255.7	A	2700	5.72	5.98	6.07	6.14	6.18	6.21	6.24
		B	2697	6.02	6.29	6.38	6.44	6.48	6.50	6.52
bqg	263.7	A	2718	5.84	6.02	6.11	6.18	6.22	6.25	6.27
		B	2723	6.19	6.31	6.38	6.44	6.47	6.50	6.52
bqg	268.2	A	2742	5.79	6.08	6.21	6.31	6.37	6.41	6.44
		B	2730	6.25	6.41	6.50	6.56	6.59	6.61	6.63
bqg	278.6	A	2721	5.61	5.86	5.96	6.03	6.07	6.10	6.13
		B	2716	6.06	6.35	6.47	6.53	6.57	6.60	6.62
bqg	284.4	A	2747	5.60	5.84	5.93	6.00	6.04	6.07	6.10
		B	2734	6.10	6.27	6.35	6.41	6.45	6.48	6.50
bqg	290.2	A	2781	5.53	5.77	5.87	5.95	6.00	6.03	6.06
		B	2753	6.05	6.30	6.41	6.48	6.52	6.55	6.57
gg	298.4	A	2658	5.59	5.90	6.02	6.10	6.15	6.18	6.21
		B	2651	5.85	6.18	6.28	6.34	6.37	6.39	6.41
gg	304.2	A	2669	5.70	5.96	6.05	6.12	6.16	6.19	6.21
		B	2661	5.99	6.23	6.31	6.36	6.40	6.42	6.44

Velocities are in kilometers per second; gg, granitic gneiss; bqg, biotite quartzofeldspathic gneiss; ag, amphibolite gneiss.

Author's Personal Copy

flow anomalies. An example is the Surrency Bright Spot in Georgia [*Brown et al.*, 1987]. It is possible that this and other deep crustal bright spots originate from deep crustal fluids [e.g., *Jones and Nur*, 1984; *Matthews and Cheadle*, 1986]. Within the continental crust, progressive metamorphism proceeds by a sequence of reactions involving dehydration. High pore pressures in fluid-filled fractures originating from the metamorphic dewatering dramatically lowers seismic velocities in crystalline rocks [*Christensen*, 1989]. Thus strong reflections could originate in midcrustal regions containing complex distributions of fluid-filled fractures.

An additional source of strong reflections originating in the deep continental crust is suggested from the synthetic seismograms generated for the Inner Piedmont section. With the exception of reflectivity models generated from velocity data below 100 MPa, where microcracks have a strong contribution to velocity [e.g., *Birch*, 1960], reflectivity synthetics at different pressures are quite similar to the modeling shown in Figure 4. An exception is at 600 MPa (Figure 10), where amplitudes are significantly higher than at other pressures and greater than the reference trace generated by an interface with a 0.1 reflection coefficient. Amplitudes at several pressures are compared in Figure 11 for synthetics generated from a program which includes multiple reflections in the modeling. Note again the strong reflections at 600 MPa.

The "bright spot" observed at 600 MPa is attributed to fine tuning of the metamorphic layering. The pressure derivatives of the velocities of individual layers are slightly different from one another. The pressure derivatives of velocities also vary with pressure. Thus, at certain pressures the combination of velocities, density, and layer thicknesses are optimum for producing major reflections. Changes in temperature with depth are also likely to be important in producing strong reflections. Values of $(\partial Vp/\partial T)_p$ at lower crustal confining pressures are -0.39 x 10^{-3} and -0.55 x 10^{-3} km s^{-1} °C^{-1} for granite and amphibolite, respectively [*Christensen*, 1979]. This significant difference in temperature derivatives of velocity suggests that lower crustal regions with interlayered silicic and mafic rocks similar to the Inner Piedmont section also have temperature-related bright spots. It is concluded that local strong reflections from the deep continental crust may originate from temperature- and pressure-related fine layer tuning of high-grade metamorphic rocks.

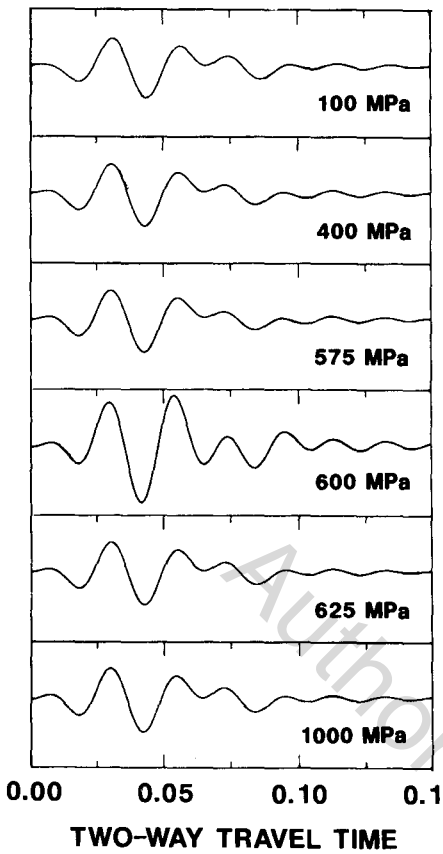

Fig. 11. A comparison of Inner Piedmont reflection synthetics at various pressures illustrating the high-amplitude reflections at confining pressures of 600 MPa.

SEISMIC ANISOTROPY OF THE DEEP CRUST

In addition to the origin of crustal reflections, an equally intriguing problem is that of the nature of lower crustal seismic anisotropy. Is seismic anisotropy an important property of the continental crust? If the crust is anisotropic, what is the symmetry? Can crustal anisotropy be readily detected by modern seismic techniques?

The overall seismic anisotropy of the complete Inner Piedmont section can be estimated from the anisotropies and thicknesses of

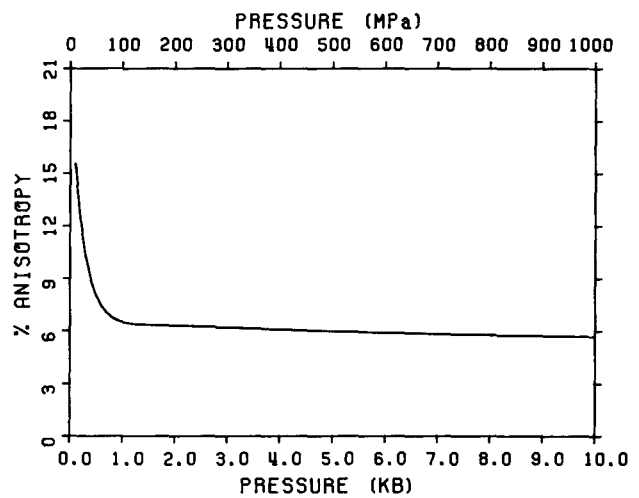

Fig. 12. Percent anisotropy versus pressure for the Inner Piedmont section.

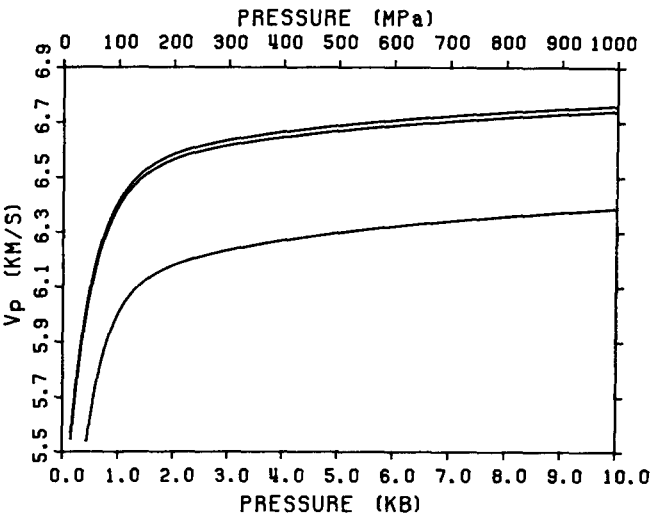

Fig. 13. Inner Piedmont section velocities for three mutually perpendicular directions. The slow velocity is for vertical propagation through the observed drill core sequence of granitic gneiss, biotite quartzofeldspathic gneiss, and amphibolite, whereas the fast velocity is horizontal and parallel to lineation.

the layers used for the reflectivity synthetics. The percent anisotropy, defined as the difference between the maximum and minimum velocities of a sample expressed as a percentage of the mean, for the Inner Piedmont section is shown in Figure 12 as a function of pressure. At low pressures, anisotropy is enhanced by oriented microcracks. At pressures above 100 MPa, the anisotropy, which is approximately 6%, originates primarily from preferred orientation of amphibole, mica, and quartz.

Plots of velocity versus pressure for three mutually perpendicular directions in the Inner Piedmont section are shown in Figure 13. The lowest velocities (~ 6.4 km/s at 1 GPa) occur for vertical propagation in the horizontally layered metamorphic sequence. Velocities are high in horizontal directions and reach 6.8 km/s at 1 GPa corresponding to a depth of approximately 35 km. Horizontally propagating waves are slightly faster parallel to lineations; however, the anisotropy in a horizontal plane is less

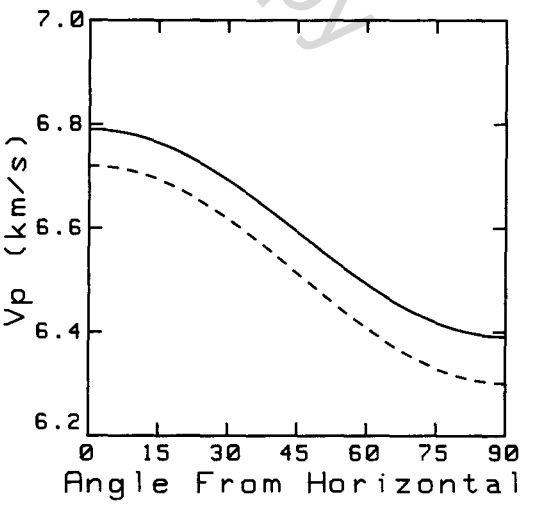

Fig. 14. Average compressional wave velocity of the Inner Piedmont section versus propagation direction within a vertical plane at pressures of 1 GPa (solid curve) and 0.5 GPa (dashed curve).

Author's Personal Copy

TABLE 3. Chemical Analyses of Inner Piedmont Samples

	Sample												
	gg	gg	ag	ag	gg	ag	ag	gg	gg	bqg	bqg	gg	Total Section[a]
Depth,m	41.8	58.2	86.0	116.7	135.0	159.7	186.8	209.1	227.7	255.7	290.2	304.2	
SiO_2	75.80	73.50	51.80	53.50	76.70	51.50	49.90	74.40	72.80	73.30	65.20	75.40	67.30
TiO_2	0.06	0.15	0.89	0.86	0.07	0.58	0.38	0.08	0.15	0.21	0.42	0.18	0.2
Al_2O_3	13.20	14.60	15.50	15.40	12.40	15.00	16.00	14.40	14.70	13.60	15.00	13.30	14.30
Fe_2O_3[b]	1.48	1.19	13.20	12.30	2.08	13.30	7.24	0.67	1.34	2.72	6.27	1.87	4.31
MnO	0.12	0.05	0.30	0.27	0.12	0.24	0.17	0.03	0.05	0.07	0.15	0.05	0.13
MgO	0.07	0.38	5.44	4.74	0.05	4.82	8.64	0.25	0.53	0.74	1.82	0.40	2.42
CaO	2.07	2.43	7.80	7.84	1.66	10.10	14.50	2.05	2.34	3.35	5.91	2.54	5.41
Na_2O	4.38	5.01	2.93	3.69	4.81	2.88	2.17	4.74	5.42	4.36	2.69	4.47	3.99
K_2O	2.60	2.28	1.14	1.19	1.85	0.67	0.33	3.16	1.83	1.21	1.90	1.66	1.64
P_2O_5	0.06	0.15	0.89	0.86	0.07	0.58	0.38	0.08	0.15	0.21	0.42	0.04	0.04
H_2O[c]	0.08	0.39	1.23	0.39	0.23	0.93	0.62	0.39	0.70	0.47	0.70	0.23	0.43
TOTAL	100.00	100.20	100.40	100.30	100.10	100.10	100.10	100.40	100.00	100.20	100.20	100.20	100.20
	Normative												
Q	35.50	29.70	2.55	1.85	37.30	2.41	1.95	30.00	28.20	34.50	25.50	36.50	23.00
Or	15.40	13.50	6.74	7.03	10.90	3.96	18.40	18.70	10.80	7.15	11.20	9.81	9.69
Ab	37.10	42.40	24.80	31.20	40.70	24.40	32.90	40.10	45.90	36.90	22.80	37.80	33.80
An	8.68	10.60	25.80	21.90	6.78	26.00	31.10	8.68	10.40	14.00	23.20	11.30	16.30
Di	1.28	0.98	9.98	13.60	1.17	19.60	3.96	1.07	0.91	1.95	4.59	0.86	8.38
Hy	1.15	1.56	21.80	17.30	1.78	15.90	7.24	0.72	2.13	3.54	8.50	2.35	6.29
Mt	0.54	0.42	4.53	4.22	0.74	4.54	2.49	0.24	0.47	0.94	2.15	0.64	1.49
11	0.11	0.28	1.69	1.63	0.13	1.10	0.72	0.15	0.28	0.40	0.80	0.34	0.51
AP	0.05	0.09	0.30	0.21	0.05	0.16	0.09	0.07	0.05	0.12	0.21	0.09	0.09

Samples are gg, granitic gneiss; bqg, biotite quartzofeldspathic gneiss; ag, amphibolite gneiss.

[a] Calculated from 10.7% 41.8, 19.9% 58.2, 1.7% 86.0, 7.9% 116.7, 15.0% 135.0, 3.1% 159.7, 17.4% 186.8, 3.7% 209.1, 1.6% 227.7, 8.8% 255.1, 5.9% 290.0, 4.3% 304.2.

[b] All Fe expressed as Fe_2O_3.

[c] Includes H_2O^+ and H_2O^-.

Author's Personal Copy

than 1% and thus is unlikely to be observed in seismic refraction surveys.

Many seismic investigations have reported 6.8 km/s velocities within the lower continental crust [e.g., *Pakiser*, 1963; *Meissner*, 1986; *Mooney and Brocher*, 1987]. A summary in histogram form of more than 200 compressional wave velocities of deep crustal refractors by *Christensen and Fountain* [1975] shows a strong peak in velocities between 6.7 and 6.8 km/s. *Pavlenkova* [1979], in her compilation of the generalized seismic structure of the continental crust, finds velocities of 6.8 km/s at crustal depths of 35-40 km in platform regions. The 6.8 km/s velocities coincide with a marked increase in the number of crustal reflections [*Pavlenkova*, 1979, Figure 3].

Lower crustal velocities determined from wide-angle analysis of reflected phases in the crust will not record maximum velocities, since wide-angle reflections do not have horizontal travel paths like that of head wave refracted arrivals. Compressional wave velocity as a function of the angle between the propagation direction and the horizontal is shown in Figure 14 for pressures of 0.5 and 1.0 GPa. The velocities from Figure 13 at 0° (horizontal propagation) and 90° (vertical propagation were obtained from averaging the complete Inner Piedmont section. Velocities obtained from cores with axes at various angles to the foliation were used to estimate the shape of the curves in Figure 14. Note that velocity is not a linear function of the angle from the horizontal and velocities determined from wide-angle reflections still will be relatively high (~ 6.7 km/s at 1 GPa) for seismic energy propagating 30° from the horizontal.

The anisotropy of the Inner Piedmont section, as well as the metamorphic layering responsible for the high reflectivity, likely originate from ductile deformation in the lower crust [*Phinney and Jurdy*, 1979; *McCarthy*, 1986; *Smithson*, 1986; *Christensen and Szymanski*, 1988]. The protolith probably was an assemblage of graywackes, volcaniclastics, and basaltic sills and dikes, now metamorphosed to biotite quartzofeldspathic gneisses and amphibolites. Horizontal extension or contraction in the lower crust, accompanied by ductile deformation and intrusion of granitic sills, produced the horizontally layered amphibolite facies metamorphic assemblage.

Chemical analyses of selected samples from the Inner Piedmont drill core are presented in Table 3 along with an estimate of the average chemistry of the total drill core. The average chemistry was obtained by assigning chemistry, based on the analyses in Table 3, to each of the 153 layers used for the reflection synthetics. The average chemistry of hole DH-1 has little importance in terms of equating the total analysis with a specific rock type. However, of significance is the observation that the overall SiO_2 content is 67.3%, which equates with SiO_2 contents of quartz diorites [*Le Maitre*, 1976]. This is also reflected in the relatively high normative percentages of quartz and feldspar. As was shown earlier, because of significant anisotropy, deep crustal refraction velocities approach 6.8 km/s for horizontal propagation in this rock assemblage. Velocities this high are usually equated with rocks of much lower SiO_2 contents, such as gabbros or mafic granulites [e.g., *Birch*, 1958; *Pakiser and Robinson*, 1966; *Christensen and Fountain*, 1975].

SUMMARY AND CONCLUSIONS

A detailed study of the seismic properties and densities of a section of granitic gneisses, biotite quartzofeldspathic gneisses, and amphibolites from the Inner Piedmont of the Southern Appalachians can be used to clarify the interpretation of conventional deep crustal reflection and refraction data. Essential to the study has been the continuous coring of a major section of high-grade metamorphic rocks, which has provided unweathered samples for a large number of laboratory measurements and the necessary stratigraphic control for the generation of reflection synthetics. Conclusions pertaining to deep crustal seismic properties, based on velocity and density data from 150 samples, petrographic observations, chemical analyses, and synthetic reflection modeling are as follows:

1. Reflections from the deep continental crust are likely to originate from a subhorizontal layering of metamorphic rocks of different seismic impedances.

2. Lower crustal bright spots can be induced by fine tuning of metamorphic layers, which is temperature and pressure related. Some caution in applying this interpretation to lower crustal bright spots is needed, however, since amplitude changes may also be caused by lateral changes in lithology, high pore pressure, and partial melting.

3. Anisotropy inherent to deep crustal metamorphic rocks similar to those of the Inner Piedmont section decreases acoustic impedance contrasts at lithologic contacts and hence reflection amplitudes.

4. The calculation of a reflection synthetic for a deep crustal rock sequence requires extremely detailed stratigraphic and lithologic control, which in most metamorphic provinces is offered only by continuous drill core. Interpretations based on reflectivity synthetics calculated from velocity measurements of a limited number of outcrop samples are to be viewed with caution.

5. Lower crustal reflections are unlikely to originate from contacts between units often shown on geologic maps of high grade metamorphic terranes. Instead, reflections originate within major map units from juxtaposition of layers of a variety of rock types with contrasting acoustic impedances. Within the Inner Piedmont section, high impedance contrasts occur at amphibolite-granite gneiss and amphibolite-biotite quartzofeldspathic gneiss contacts.

6. Crustal regions that have undergone ductile flow are likely to have significant seismic anisotropy produced by preferred mineral orientation. However, because of symmetry considerations, the anisotropy is unlikely to be detected by standard refraction techniques. Velocities in a horizontal plane will not vary greatly with azimuth but are much higher than vertical velocities. Because of anisotropy, reflection and refraction depths will not coincide.

7. Correlations of deep crustal refraction velocities with petrology and chemistry are complicated by anisotropy. The lower crust may have a higher SiO_2 content than has been previously estimated.

Acknowledgments. The laboratory studies were supported by the Office of Naval Research contract N00014-89-J-1209. R.D. Hatcher, Jr. and R.T. Williams provided samples of the core which was drilled with funding from National Science Foundation grant EAR8417894. H. Benz calculated the synthetics of Figure 11, and R. Smith provided computer facilities at the University of Utah for the calculations. J. Costain and C. Coruh provided a preprint of the reflection data. The assistance of D. Ballotti, D. Szymanski, and W. Wepfer is greatly appreciated. J. McCarthy and S. Smithson provided constructive reviews of the manuscript.

REFERENCES

Birch, F., Interpretation of the seismic structure of the crust in light of experimental studies of wave velocities in rocks, in *Contributions in Geophysics in Honor of Beno Gutenberg*, edited by H. Benioff, pp. 158-170, Pergamon, New York, 1958.

Birch, F., The velocity of compressional waves in rocks to 10 kilobars, 1, *J. Geophys. Res.*, *65*, 1083-1102, 1960.

Blundell, D.J., and B. Raynaud, Modeling lower crust reflections observed on BIRPS profiles, in *Reflection Seismology: A Global Perspective*, *Geodyn. Ser.*, vol. 13, edited by M. Barazangi and L. Brown, pp. 287-295, AGU, Washington, D.C., 1986.

Bois, C., M. Cazes, A. Hirn, P. Matte, A. Mascle, L. Montadert, and B. Pinet, Crustal laminations in deep seismic profiles in France and neighboring areas, *Geophys. J.R. Astron. Soc.*, *89*, 297-304, 1987.

Brown, L., C. Chapin, A. Sanford, S. Kaufman, and J. Oliver, Deep structure of the Rio Grande rift from seismic reflection profiling, *J. Geophys. Res.*, *85*, 4773-4800, 1980.

Brown, L.D., et al., COCORP: New perspectives on the deep crust, *Geophys. J.R. Astron. Soc.*, *89*, 47-54, 1987.

Christensen, N.I., Compressional wave velocities in metamorphic rocks at pressures to 10 kbar, *J. Geophys. Res.*, *70*, 6147-6164, 1965.

Christensen, N.I., Compressional wave velocities in rocks at high temperatures and pressures, critical thermal gradients, and crustal low velocity zones, *J. Geophys. Res.*, *84*, 6849-6857, 1979.

Christensen, N.I., Pore pressure, seismic velocities and crustal structure, Geophysical Framework of the United States, edited by L. Pakiser and W. Mooney, *Mem. Geol. Soc. Am.*, in press, 1989.

Christensen, N.I., and D.M. Fountain, Constitution of the lower continental crust based on experimental studies of seismic velocities in granulite, *Geol. Soc. Am. Bull.*, *86*, 227-236, 1975.

Christensen, N.I., and D.L. Szymanski, Origin of reflections from the Brevard fault zone, *J. Geophys. Res.*, *93*, 1087-1102, 1988.

Coruh, C., J.K. Costain, R.D. Hatcher, Jr., T.L. Pratt, R.T. Williams, and R.A. Phinney, Results from regional vibroseis profiling: Appalachian ultradeep core hole site study, *Geophys. J.R. Astron. Soc.*, *89*, 147-155, 1987.

Costain, J.K., R.D. Hatcher, Jr., and C. Coruh, Appalachian ultradeep core hole (ADCOH) project site investigation regional seismic lines and geologic interpretation, in *The Geology of North America-An Overview*, vol. A., Geological Society of America, Boulder, Colo., in press, 1989.

Coward, M.P., Flat lying structures within the Lewisian basement gneiss complex of NW Scotland, *Proc. Geol. Assoc.*, *85*, 459-572, 1973.

Farrar, S., A. Stieve, and J. Hopson, Hole #1 core descriptions, in *Appalachian Ultradeep Core Hole (ADCOH) Project Site Investigation Data Set 1*, *Stud. Geol.*, vol. 17, edited by J.L. Hopson and R.D. Hatcher, Jr., pp. 47-68, Department of Geological Sciences, University of Tennessee at Knoxville, 1986.

Fuchs, K., On the properties of deep crustal reflectors, *Z. Geophys.*, *35*, 133-149, 1969.

Goodwin, E.B., and G.A. Thompson, The seismically reflective crust beneath highly extended terranes: Evidence for its origin in extension, *Geol. Soc. Am. Bull.*, *100*, 1616-1626, 1988.

Hale, L.D., and G.A. Thompson, The seismic reflection character of the continental Mohorovicic discontinuity, *J. Geophys. Res.*, *87*, 4625-4635, 1982.

Hatcher, R.D., Jr., J.K. Costain, C. Coruh, R.A. Phinney, and R.T. Williams, Tectonic implications of new Appalachian Ultradeep Core Hole (ADCOH) seismic reflection data from the crystalline southern Appalachians, *Geophys. J.R. Astron. Soc.*, *89*, 157-169, 1987.

Hurich, C.A., and S.B. Smithson, Compositional variation and the origin of deep crustal reflections, *Earth Planet. Sci. Lett.*, *85*, 416-426, 1987.

Hurich, C.A., S.B. Smithson, D.M. Fountain, and M.C. Humphreys, Seismic evidence of mylonite reflectivity and deep structure in the Kettle dome metamorphic core complex, Washington, *Geology*, *13*, 577-580, 1985.

Jones, T.D., and A. Nur, The nature of seismic reflections from deep crustal fault zones, *J. Geophys. Res.*, *89*, 3153-3171, 1984.

Le Maitre, R.W., The chemical variability of some common igneous rocks, *J. Petrol.*, *17*, 589-637, 1976.

Matthews, D.H., and M.J. Cheadle, Deep reflections from the Caledonides and Variscides west of Britain and comparison with the Himalayas, in *Reflection Seismology: A Global Perspective*, *Geodyn. Ser.*, vol. 13, edited by M. Barazangi and L. Brown, pp. 5-20, AGU, Washington, D.C., 1986.

McCarthy, J., Reflection profiles from the Snake River metamorphic core complex: a window into the mid-crust, in *Reflection Seismology: The*

Continental Crust, Geodyn. Ser., vol. 14, edited by M. Barazangi and L. Brown, pp. 281-292, AGU, Washington, D.C., 1986.

Meissner, R., *The Continental Crust, A Geophysical Approach*, 428 pp., Academic, San Diego, Calif., 1986.

Mooney, W.D., and T.M. Brocher, Coincident seismic reflection/refraction studies of the continental lithosphere: A global review, *Rev. Geophys., 25*, 723-742, 1987.

Newton, R.C., Petrologic aspects of Precambrian granulite facies terrains bearing on their origins, in *Proterozoic Lithospheric Evolution, Geodyn. Ser.*, vol. 17, edited by A. Kroner, pp. 11-26, AGU, Washington, D.C., 1987.

Ostrander, W.J., Plane-wave reflection coefficients for gas sands at non normal angles of incidence, *Geophysics, 49*, 1637-1648, 1984.

Pakiser, L.C., Structure of the crust and upper mantle in the western United States, *J. Geophys. Res., 68*, 5747-5756, 1963.

Pakiser, L.C., and R. Robinson, Composition and evolution of the continental crust as suggested by seismic observations, *Tectonophysics*, 3, 547-557, 1966.

Park, R., Origin of horizontal structure in Archean high grade terrains, *Spec. Publ. Geol. Soc. Aust., 7*, 481-490, 1981.

Pavlenkova, N.I., Generalized geophysical model and dynamic properties of the continental crust, *Tectonophysics, 59*, 381-390, 1979.

Percival, J.A., and K.D. Card, Archean crust as revealed in the Kapuskasing uplift, Superior Province, Canada, *Geology, 11*, 323-326, 1983.

Phinney, R.A., and D.M. Jurdy, Seismic imaging of deep crust, *Geophysics, 44*, 1637-1660, 1979.

Sandiford, M., and R. Powell, Deep crustal metamorphism during continental extension: Modern and ancient examples, *Earth Planet. Sci. Lett., 79*, 151-158, 1986.

Sheriff, R.E., Factors affecting seismic amplitudes, *Geophys. Prospect., 23*, 125-138, 1975.

Smithson, S.B., A physical model of the lower crust from North America based on seismic reflection data, The Nature of the Lower Continental Crust, edited by J.B. Dawson, D.A. Carswell, J. Hall, and K.H. Wedepohl, *Spec. Publ. Geol. Soc. Am., 24*, 23-24, 1986.

Smithson, S.B., R.A. Johnson, and C.A. Hurich, Crustal reflections and crustal structure, in *Reflection Seismology: The Continental Crust, Geodyn. Ser.*, vol. 14, edited by M. Barazangi and L. Brown, 21-32, AGU, Washington, D.C., 1986.

Velzeboer, C.J., The theoretical seismic reflection response of sedimentary sequences, *Geophysics, 46*, 843-853, 1981.

Widess, M.B., How thin is a thin bed?, *Geophysics, 38*, 1176-1180, 1973.

Williams, R.T., R.D. Hatcher, Jr., C. Coruh, J.K. Costain, M.D. Zoback, R.N. Anderson, J.B. Diebold, and R.A. Phinney, The southern Appalachian ultradeep scientific drill hole: Progress of site location investigations and other recent developments, in *Observation of the Continental Crust through Drilling II*, edited by H.J. Behr, F.G. Stehli and H. Vidal, pp. 44-55, Springer-Verlag, New York, 1987.

N. I. Christensen, Department of Earth & Atmospheric Sciences, Purdue University, West Lafayette, IN 47907.

(Received February 21, 1989;
revised September 18, 1989;
accepted September 7, 1989.)

Author's Personal Copy